

Hydrodynamic response in AMPT simulations

De-Xian Wei and Xu-Guang Huang*

*Department of Physics and Center for Field Theory and Particle Physics,
Fudan University, Shanghai, 200433, China and*

Key Laboratory of Nuclear Physics and Ion-beam Application (MOE), Fudan University, Shanghai 200433, China

Li Yan†

Department of Physics, McGill University 3600 rue University Montréal, QC Canada H3A 2T8

We carry out simulations using A Multi-Phase Transport (AMPT) model to describe the observed flow signatures in the $\sqrt{s_{NN}} = 2.76$ TeV Pb-Pb collisions. Especially, we calculate the flow fluctuations of v_2 in terms of cumulant ratios and the standardized skewness. Based on event-by-event AMPT simulations, we study the linear and cubic response relation between v_2 and ε_2 . We found that the observed response relation is compatible to what has been noticed in hydrodynamic modelings, with similar dependence on shear viscosity. Besides, this response relation is not sensitive to non-flow effect.

I. INTRODUCTION

One remarkable achievement in high-energy heavy-ion experiments is the creation of a fluid-like quark-gluon system – the Quark-Gluon Plasma (QGP). At RHIC and the LHC energies, it has been realized that the physics of the created QGP medium can be understood in terms of relativistic viscous hydrodynamics (see [1] for a recent review), with extremely small dissipative corrections. For instance, simulations based on hydrodynamic modelings of the QGP medium evolution provide so far the best description of the so-called harmonic flow V_n , and correlations and fluctuations of these flow [2–5], given an input of the specific shear viscosity (shear viscosity over entropy density ratio) close to a lower theoretical bound $\eta/s = \hbar/4\pi k_B$ [6].

Harmonic flow V_n characterizes the azimuthal anisotropy of the generated particle spectrum in momentum space [7, 8]. For each collision event, with respect to the probability distribution of the generated particles in azimuthal angle, $f(\phi_p)$, one defines V_n as

$$V_n = v_n e^{in\Psi_n} \equiv \int \frac{d\phi}{2\pi} e^{in\phi_p} f(\phi_p). \quad (1)$$

The parameter n denotes harmonic order, with $n = 2$ corresponding to elliptic flow, $n = 3$ corresponding to triangular flow, etc. Note that V_n is a complex quantity by definition, which depends in principle on particle species, transverse momentum, pseudo-rapidity, etc. On an event-by-event basis, both its magnitude v_n , and phase, Ψ_n , fluctuate. Correlations and fluctuations of V_n determine all kinds of the measured flow signatures in experiments, such as the cumulants of flow and event-plane correlations [9].

Hydrodynamic modelings of heavy-ion collisions have lead to a set of response relations between V_n and the

fluctuating initial-state geometry of the colliding systems. More precisely, these relations are written in terms of initial state eccentricity \mathcal{E}_n , which is defined with respect to the initial-state energy density profile $\rho(\vec{x}_\perp, \tau_0)$ as [10]¹

$$\mathcal{E}_n = \varepsilon_n e^{in\Phi_n} \equiv - \frac{\int d^2\vec{x}_\perp \rho(\vec{x}_\perp, \tau_0) r^n e^{in\phi}}{\int d^2\vec{x}_\perp r^n \rho(\vec{x}_\perp, \tau_0)}. \quad (2)$$

Note that, since $|\mathcal{E}_n| = \varepsilon_n < 1$ by definition, harmonic flow V_n can be expanded with respect to \mathcal{E}_n , and a series of response relation can be obtained. A recent review on these response relations can be found in Ref. [11]. Although the response relation for V_2 and similar response relations for higher order flow are empirical based on event-by-event hydrodynamic simulations, they are conceptually compatible with the physics of hydrodynamic response theory. In particular, one may understand these response as evolution of long-wavelength hydrodynamic modes, in the way that the response coefficients solely depend on the medium dynamical properties. Therefore, in one selected centrality class where system multiplicity is roughly constant, fluctuations of these response coefficients can be ignored. In recent experiments, information of the flow correlations and fluctuations have been achieved with high precisions, from which, hydrodynamic response relations can be examined [12–15].

Although hydrodynamic response relations are well-established in hydrodynamic modelings, it is of interest to analyze these relations beyond hydrodynamics. In particular, one notices that non-flow effects result in additional event-by-event fluctuations, which are not characterized in hydrodynamics. In this work, by simulations based on a Multi-Phase Transport (AMPT) model [16],

¹ For $n = 1$, the dipolar anisotropy is defined as

$$\mathcal{E}_1 = \varepsilon_1 e^{in\Phi_1} \equiv - \frac{\int d^2\vec{x}_\perp \rho(\vec{x}_\perp, \tau_0) r^3 e^{i\phi}}{\int d^2\vec{x}_\perp r^3 \rho(\vec{x}_\perp, \tau_0)}$$

* huangxuguang@fudan.edu.cn

† li.yan@physics.mcgill.ca

we re-examine the hydrodynamic response relation between V_2 and \mathcal{E}_2 . This paper is organized as follows: In Section II we briefly describe the AMPT model and parameters used in the present simulations. Flow signatures are obtained correspondingly by correlating generated particles. In particular, fluctuations of v_2 are studied in terms of flow cumulants. Hydrodynamic response relation for v_2 is detailed in Section III, where we emphasize its dependence on shear viscosity and non-flow effects. Throughout this paper, our results and analyses are mostly obtained based on AMPT simulations with respect to Pb-Pb collisions at $\sqrt{s_{NN}} = 2.76$ TeV at the LHC. Similar results of the recent $\sqrt{s_{NN}} = 5.02$ TeV Pb-Pb collisions are presented in Appendix A. We will use natural unit $k_B = c = \hbar = 1$.

II. AMPT AND HEAVY-ION COLLISIONS

The AMPT model is a hybrid model in which QGP evolution in heavy-ion collisions is described by parton scatterings [16]. In AMPT model, the initial-state particle distributions are generated by HIJING model [17]. For the current study, string melting is considered so that the produced hadrons from HIJING model are further converted into valence quarks and anti-quarks. Right before parton scatterings, we record the generated energy density profile of the system $\rho(\vec{x}, \tau_0)$, as the initial state of medium evolution. Initial state eccentricities of each event are then calculated with respect to Eq. (2). Parton scatterings, and accordingly the space-time evolution of QGP, are determined via ZPC parton cascade model [18], with the differential cross-section

$$\frac{d\sigma}{dt} \approx \frac{9\pi\alpha_s^2}{2(t - \mu^2)^2}. \quad (3)$$

In the above equation, α_s is the strong coupling constant, t is the Mandelstam variable, and μ is the screening mass in the partonic system. These parameters are adjustable according to colliding systems so that measurable quantities in experiments, such as total yields, elliptic flow v_2 , and two-pion correlations, can be reproduced. For later convenience, we also notice the following relation [19],

$$\frac{\eta}{s} \approx \frac{3\pi}{40\alpha_s^2} \frac{1}{\left(9 + \frac{\mu^2}{T^2}\right) \ln\left(\frac{18 + \mu^2/T^2}{\mu^2/T^2}\right) - 18}, \quad (4)$$

which allows one to estimate the specific shear viscosity η/s in terms of partonic differential cross-section. Note that an increasing running coupling α_s leads to smaller η/s . Equation (4) represents a temperature dependent estimate, as long as screen mass μ is not linear in temperature [20]. In this work, we shall consider a constant screening mass, which results in a rise of η/s when temperature decreases. In AMPT model, quarks and anti-quarks combine to form hadrons via a spatial coalescence model when scatterings stop. Hadronic phase of the system evolves according to a relativistic transport model until hadrons freeze-out.

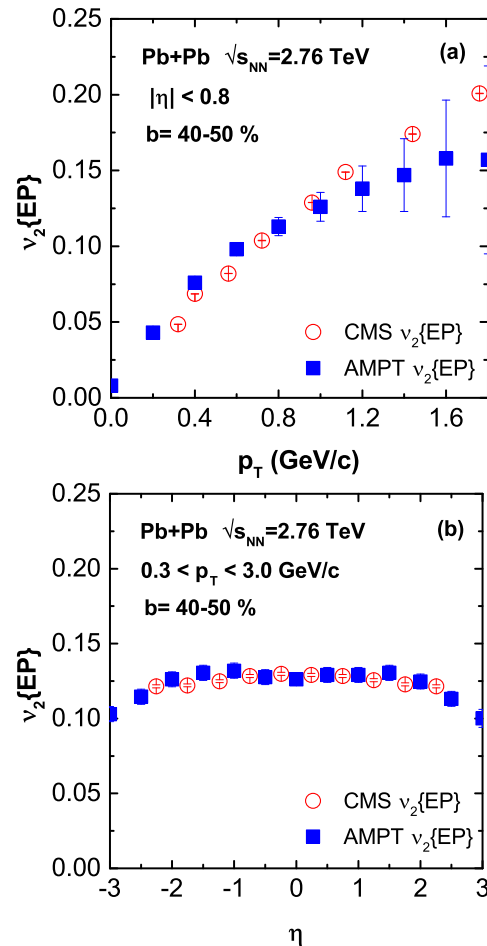


FIG. 1. (Color online) The (a) p_T - and (b) η - dependent elliptic flow v_2 measured with respect to the event plane in the 40 - 50% centrality class. Blue symbols are obtained from AMPT simulations, in comparison with the CMS data at $\sqrt{s_{NN}} = 2.76$ TeV [21].

Although in each single event only a finite number of particles are produced, the probability distribution of these particles in azimuthal angle $f(\phi_p)$ can still be estimated, from which one can obtain the complex flow harmonics V_n using definition Eq. (1). This complex V_n in each event suffers from statistical uncertainty due to finite number effect. A more systematic way to calculate flow harmonics is to correlate particles from all events in one centrality class, as has been done in experiments. From two-particle correlations, one obtains $v_n\{2\}$. From four-, six-, and eight-particle correlations, one obtains higher order cumulants of flow harmonics: $v_n\{4\}$, $v_n\{6\}$ and $v_n\{8\}$. An estimate of the event plane in the collisions can be done in a similar manner, and correspondingly one has the flow harmonics measured with respect to the event plane $v_n\{EP\}$.

By choosing appropriate parameters in the AMPT model according to Ref. [19], we are able to reproduce the measured observables at the LHC. For instance, the

differential elliptic flow $v_2\{EP\}$ as a function of p_T and pseudo-rapidity are shown in Fig. 1 for the centrality class 40-50% of Pb-Pb collisions at $\sqrt{s_{NN}} = 2.76$ TeV, with good agreements observed comparing to the CMS results. In these calculations, in addition to parameters that control the Lund string fragmentation, $a = 0.5$ and $b = 0.9$ GeV $^{-2}$, $\alpha_s = 0.33$ and $\mu = 3.2$ fm $^{-1}$ are chosen, so that effectively one has a relatively large specific shear viscosity. At the initial temperature of LHC Pb-Pb collisions at $\sqrt{s_{NN}} = 2.76$ TeV which is around $T \approx 468$ MeV obtained by estimating the initial energy density, one effectively has $\eta/s = 0.273$ in the deconfined system.

In recent experiments at the LHC energies, more sophisticated measurements of elliptic flow have been carried out, revealing the fluctuating nature of v_2 (cf Ref. [22–24]). To estimate the fluctuation effect of v_2 , for the Pb-Pb collisions at $\sqrt{s_{NN}} = 2.76$ TeV, in each 5%-centrality bin from the 15% to 60%, we generate approximately 5000 events from AMPT simulations. In Fig. 2, our AMPT results for the ratio of $v_2\{6\}/v_2\{4\}$ and ratio $v_2\{8\}/v_2\{4\}$ are presented as colored bands as a function of centrality percentile. The width of bands corresponds to statistical errors due to finite number effect, which in our calculations are estimated via a jackknife resampling. In comparison to the experiments from the ALICE collaboration (red points), an overall agreement is observed within errors, which indicates that AMPT model is able to capture the non-Gaussian properties of v_2 fluctuations.

One should be aware that both ratios are less than unity, and also the fact that $v_2\{8\}$ is smaller than $v_2\{6\}$, are characteristic natures of flow fluctuations known from hydrodynamic modeling. In hydrodynamic modeling of heavy-ion collisions, fluctuations of elliptic flow v_2 are mostly determined by fluctuations of initial ellipticity ε_2 , due to the fact that $V_2 \propto \mathcal{E}_2$. This is also observed in our AMPT calculations. As shown in Fig. 2 the ratio of cumulants of ε_2 (blue squares) are compatible with those of v_2 , except for very peripheral collisions where the ratios of ε_2 are slightly larger.

The information of v_2 fluctuations can be as well captured by skewness. Given $v_2\{2\}$, $v_2\{4\}$ and $v_2\{6\}$, one may estimate the standardized skewness as [14]

$$\gamma^{expt} \equiv -6\sqrt{2}v_2\{4\}^2 \frac{v_2\{4\} - v_2\{6\}}{[v_2\{2\}^2 - v_2\{4\}^2]^{3/2}}. \quad (5)$$

Fig. 3 depicts the estimated standardized skewness of v_2 fluctuations from our AMPT simulations, as colored bands. Again, width of the band is determined by statistical errors via a jackknife resampling. AMPT results agree well with the recent experimental data (red points). One observes a negative value of the skewness, with its magnitude increases as centrality percentile grows. In hydrodynamic modeling, this negative skewness of v_2 fluctuations is understood as a consequence of the negative skewness of ε_2 , due to the combined effect of an upper bound $\varepsilon_2 < 1$ and a non-zero mean of ellipticity in the reaction plane. Similarly, we notice that in the case of

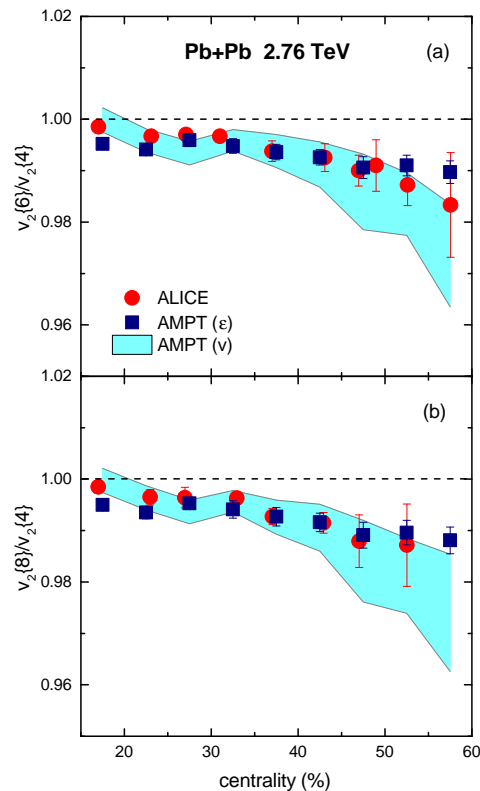


FIG. 2. (Color online) Ratios of cumulants (a) $v_2\{6\}/v_2\{4\}$ and (b) $v_2\{8\}/v_2\{4\}$. Red points are from ALICE collaboration [24], colored bands are results of AMPT calculations. The corresponding cumulant ratios of initial ellipticity ε_2 are shown as blue squares.

AMPT simulations, skewness of v_2 is comparable with that of initial ε_2 .

III. HYDRODYNAMIC RESPONSE RELATION IN AMPT

In the previous section we have seen v_2 fluctuations from AMPT simulations, in terms of cumulant of v_2 from multi-particle correlations and standardized skewness. Especially, the fluctuations of v_2 follow to a large extent the fluctuations of ε_2 . This feature is very similar to what one would expect in a hydrodynamic modeling of heavy-ion collisions, in which a hydrodynamic response relation between V_2 and \mathcal{E}_2 has been established [25],

$$V_2 = \kappa_2 \mathcal{E}_2 + \kappa'_2 \varepsilon_2^2 \mathcal{E}_2 + \delta_2 \quad (6)$$

Equation (6) is achieved by regarding initial state eccentricity ε_n as small quantities, hence one may expand the complex quantities V_2 in terms of \mathcal{E}_n . Owing to the condition of rotational symmetry, the leading order term is a linear response proportional to \mathcal{E}_2 , with κ_2 the linear response coefficient determined by medium dynamical expansion. The next leading order contribution is

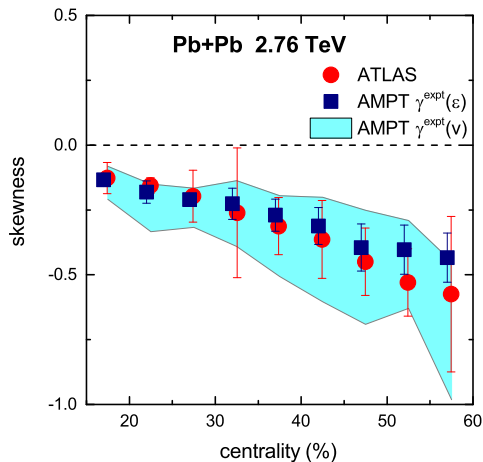


FIG. 3. (Color online) Standardized skewness of v_2 fluctuations in Pb-Pb collisions as a function of centrality from AMPT simulations (colored band) and ATLAS [14] data (red points). The corresponding results of standardized skewness of initial state ε_2 is shown as blue squares.

of cubic order, and is dominantly determined by $O(\varepsilon_2^3)$. Apparently, the cubic order contribution is not important unless ε_2 becomes large, as in peripheral collisions. The quantity δ_2 in Eq. (6) describes additional event-by-event fluctuations, which affects the response relation on an event-by-event basis.

Although V_2 fluctuates from event to event, as well as \mathcal{E}_2 , both the linear response coefficient κ_2 and cubic order response coefficient κ'_2 are considered constant in each centrality class. By minimizing the effect of additional fluctuations δ_2 , one solves κ_2 and κ'_2 [25],

$$\kappa_2 = \frac{\text{Re}(\langle \varepsilon_2^6 \rangle \langle V_2 \mathcal{E}_2^* \rangle - \langle \varepsilon_2^4 \rangle \langle V_2 \mathcal{E}_2^* \varepsilon_2^2 \rangle)}{\langle \varepsilon_2^6 \rangle \langle \varepsilon_2^2 \rangle - \langle \varepsilon_2^4 \rangle^2} \quad (7a)$$

$$\kappa'_2 = \frac{\text{Re}(-\langle \varepsilon_2^4 \rangle \langle V_2 \mathcal{E}_2^* \rangle + \langle \varepsilon_2^2 \rangle \langle V_2 \mathcal{E}_2^* |\varepsilon_2|^2 \rangle)}{\langle \varepsilon_2^6 \rangle \langle \varepsilon_2^2 \rangle - \langle \varepsilon_2^4 \rangle^2}, \quad (7b)$$

where bracket $\langle \dots \rangle$ indicates average over events. Note that if one ignores contribution from cubic order response, κ_2 in Eq. (7) reduces to

$$\kappa_2 = \frac{\text{Re} \langle V_2 \mathcal{E}_2^* \rangle}{\langle \varepsilon_2^2 \rangle} \quad (8)$$

One may check that a cubic order correction reduces slightly the linear response coefficient, comparing Eq. (8) to Eq. (7).

Equation (6) in hydrodynamic modeling has been verified by event-by-event hydrodynamic simulations [5, 25, 26]. It is interesting to test the response relation in AMPT model. In the present setup of AMPT simulations for the Pb-Pb collisions at $\sqrt{s_{NN}} = 2.76$ TeV, we focus on the centrality class 45-50%. In hydrodynamic modeling, in 45-50% centrality class, both linear and non-linear response are found important. We generate approximately 5000 events in our AMPT simulations. A

scatter plot of v_2 versus ε_2 is obtained and shown Fig. 4 (d). Each point in Fig. 4 (d) corresponds to one collision event. It is worth mentioning that, the statistical uncertainty of v_2 in each event due to finite multiplicity is not included, which would in principle lead to a smearing along v_2 in Fig. 4. In Fig. 4 (d), these points distribute along a line, except for a slight tilde at large values of ε_2 which implies nonlinearity. We find that a response relation between magnitudes derived from Eq. (6), describes well the trend,

$$v_2 = \kappa_2 \varepsilon_2 + \kappa'_2 \varepsilon_2^3, \quad (9)$$

similar to what one would expect from hydrodynamics. Given these solved values of κ_2 and κ'_2 according to Eq. (7), Eq. (9) is plotted in Fig. 4 (d) as the red solid line. Without the cubic order correction, one has $v_2 = \kappa_2 \varepsilon_2$ which is shown as white dashed line in the figure. It should be emphasized that the red line and white dashed line are *not* fitting the scattering points, but determined with respect to the solved values of κ_2 and κ'_2 according to Eq. (7). Note also that the resulted linear response coefficient κ_2 are not identical with or without cubic order corrections. Dispersion around the linear and cubic order response reflects event-by-event fluctuations. Width of the dispersion is related to fluctuation strength.

A. Effect of η/s

In hydrodynamics, the effects of η/s are two-fold. First, it crucially determines medium response, *i.e.*, κ_2 and κ'_2 . When η/s increases, the linear response coefficient is suppressed. Second, from hydrodynamic simulations, it has also been noticed that event-by-event fluctuations around hydrodynamic response relations are reduced with respect to a larger value of η/s [5, 25].

To study dissipative effect in AMPT simulations, by changing parameters for the parton cascade and for the Lund string fragmentation, we adjust effectively the ratio of shear viscosity to entropy density η/s of partons, with respect to Eq. (4). We simulate AMPT model in the same centrality class (45-50%), keeping total multiplicity unchanged but varying η/s . We summarize these four sets of parameters used in AMPT simulations in Table I. In addition to set D that has been used in previous sections to describe the $\sqrt{s_{NN}} = 2.76$ TeV Pb-Pb collisions, which has, at $T = 468$ MeV, $\eta/s = 0.273$, parameter set A, B, and C lead to, at $T = 468$ MeV, $\eta/s = 0.08, 0.10$ and 0.14 respectively. Correspondingly, results with respect to these simulations are shown in Fig. 4 (a), Fig. 4 (b) and Fig. 4 (c).

For each set of η/s , we calculate linear and cubic response coefficients, κ_2 and κ'_2 , giving rise to the response relation with (red solid lines) or without (white dashed lines) cubic order corrections. As anticipated, the value of linear response coefficient, the slope of lines in Fig. 4, reduces as η/s increases, in consistency with hydrodynamic modeling of heavy-ion collisions. We plot in Fig. 5

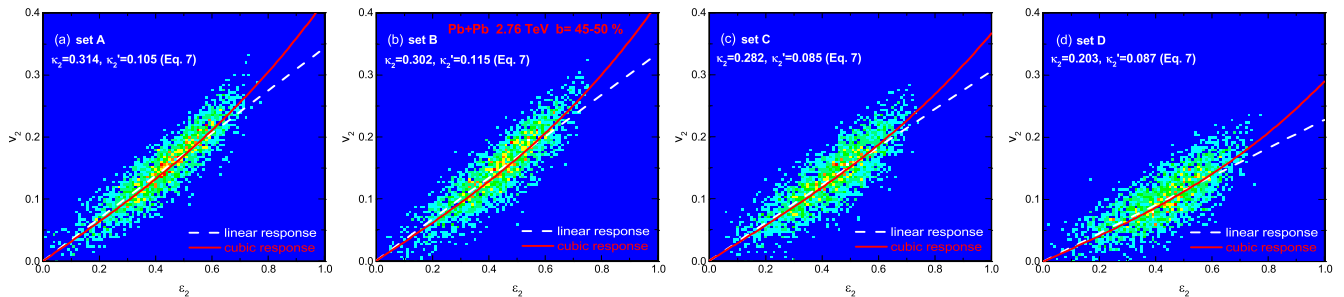


FIG. 4. (Color online) Scatter plot of event-by-event v_2 from AMPT simulations for Pb-Pb collisions, as a function of ε_2 . We take model parameters so that the effectively specific shear viscosity η/s is increased from (a) 0.08, to (b) 0.10, (c) 0.14 (d) 0.273, at temperature $T = 468$ MeV. Red solid lines are from relation Eq. (9) with a cubic order correction, while white dashed lines correspond to linear response relation.

set	A	B	C	D
η/s ($T = 468$ MeV)	0.08	0.10	0.14	0.273
a	2.2	2.2	2.2	0.5
b (GeV^{-2})	0.5	0.5	0.5	0.9
α_s	0.47	0.47	0.47	0.33
μ (fm^{-1})	1.8	2.3	3.2	3.2

TABLE I. Parameters used in AMPT simulations corresponding to different values of η/s at $T = 468$ MeV. Parameters are taken according to Ref. [27, 28].

(a) the obtained value of linear and cubic response coefficients. The cubic order response coefficient remains approximately constant, $\kappa'_2 \approx 0.1$.

In contrast to hydrodynamic modeling, the event-by-event fluctuations are not suppressed by viscosity in the AMPT simulations, as can be seen from the width of dispersion in Fig. 4. In fact, one finds a slight increase of the fluctuation strength, if it is measured relative to the mean of v_2 , $\langle |\delta_2|^2 \rangle / \langle v_2^2 \rangle$. To quantify these effects, we measure the correlation of complex variables V_2 and \mathcal{E}_2 , by the Pearson correlation coefficient,

$$C(2, 2) = \frac{\text{Re}\langle V_2 \mathcal{E}_2^* \rangle}{\sqrt{\langle v_2^2 \rangle \langle \varepsilon_2^2 \rangle}}. \quad (10)$$

The Pearson correlation coefficient $C(2, 2)$ captures simultaneously correlation between magnitudes and phases. An absolute correlation is approached when $C(2, 2) = 1$, while $C(2, 2) = 0$ indicates no correlation. Since fluctuations tend to break correlation between V_2 and \mathcal{E}_2 , effect of fluctuation reduces $C(2, 2)$. In Fig. 5 (b), we indeed find that $C(2, 2)$ decreases linearly as η/s increases from set A to set D.

B. Non-flow subtraction

We have studied the linear and cubic response which relates elliptic flow V_2 and initial ellipticity \mathcal{E}_2 via AMPT

simulations. Although the strategy is very similar to hydrodynamic simulations, with the linear and cubic order response coefficients obtained through minimizing event-by-event fluctuations, AMPT simulations contain non-flow effects. These non-flow effects are beyond pure hydrodynamic calculations, including, *e.g.*, short-ranged correlations in the deconfined medium from particle scatterings, hence they are non-hydrodynamic. Nonetheless, considering the fact that linear and cubic response relations are hydrodynamic and are dominated by the evolution of long-wavelength modes of the medium system, one would expect that the response relations depend little on non-flow effects.

In order to test the non-flow effects on the linear and cubic response, we subtract non-flow contributions in the AMPT simulations. To subtract non-flow effects in the flow harmonics, one may either take a pseudo-rapidity gap or rely on multi-particle cumulants. Both methods have been applied extensively in experiments [29–31]. Therefore, based on the response relation in Eq. (6), we find from the two-particle and four-particle correlations,

$$v_2\{2, |\Delta\eta|\} = \kappa_2 \varepsilon_2 \{2\} \left[1 + \frac{\kappa'_2 \langle \varepsilon_2^4 \rangle}{\kappa_2 \langle \varepsilon_2^2 \rangle} \right], \quad (11a)$$

$$v_2\{4\} = \kappa_2 \varepsilon_2 \{4\} \left[1 + \frac{\kappa'_2 \frac{2\langle \varepsilon_2^2 \rangle \langle \varepsilon_2^4 \rangle - \langle \varepsilon_2^6 \rangle}{2\langle \varepsilon_2^2 \rangle^2 - \langle \varepsilon_2^4 \rangle}}{\kappa_2} \right]. \quad (11b)$$

In writing Eq. (11), we have assumed that a pseudo-rapidity gap is sufficient to take out the non-flow contribution, *i.e.*, δ_2 , in $v_2\{2\}$. In practice, a pseudo-rapidity gap $|\Delta\eta| > 1$ is taken into account in our AMPT simulations for $v_2\{2, |\Delta\eta|\}$. Similarly, δ_2 does not appear in $v_2\{4\}$. Equation (11) then allows us to solve κ_2 and κ'_2 , without non-flow effects. The corresponding results of response coefficients are shown in Fig. 5 (a) as a function of η/s , and in Fig. 6 as a function of centrality percentile. As expected, numerical solutions of the response coefficients are found compatible with or without non-flow contributions.

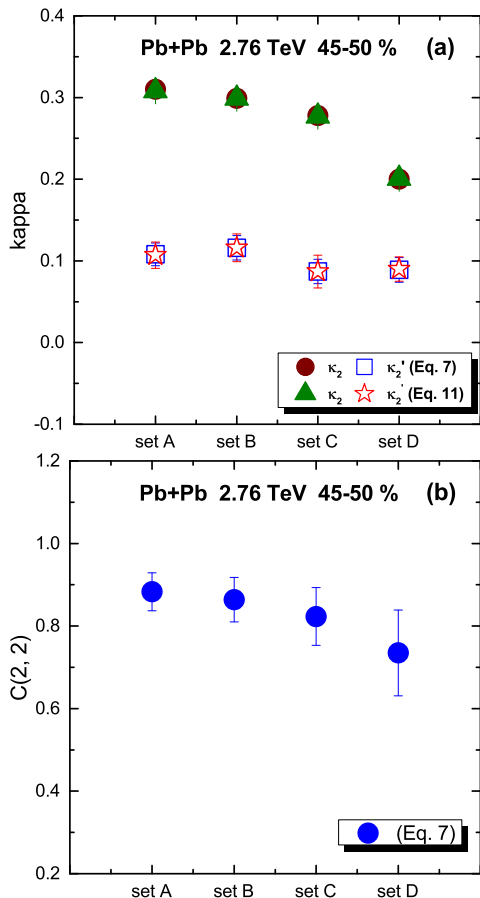


FIG. 5. (Color online) (a) AMPT results of the linear response and cubic response coefficients of the Pb-Pb 45-50% centrality class for four different sets of parameters corresponding to an increase of η/s from set A to set D, with respect to Eq. (7) and Eq. (11) with non-flow subtraction. (b) Pearson correlation coefficient $C(2,2)$ for different sets of parameters.

IV. SUMMARY AND DISCUSSIONS

In this work, we have carried out AMPT simulations for the Pb-Pb collisions at the LHC energy $\sqrt{s_{NN}} = 2.76$ TeV. Our AMPT results of elliptic flow, especially the fluctuations of v_2 are compatible with experiments. In addition, we found that the fluctuation behavior of v_2 , characterized in terms of cumulant ratios or the standardized skewness, is closely related to that of ε_2 . This feature has been noticed in hydrodynamic modelings, where the hydrodynamic response relations were proposed to explain the generation of harmonic flow. In the AMPT model, we observed very similar response relations, which can be well described by proper linear and cubic order response coefficients. This observation confirms the fact that elliptic flow v_2 is indeed a consequence of medium response to initial state ε_2 . Since the medium response reflects long-wavelength mode evolution, which is hydrodynamic, similarity to what has been found in hydro-

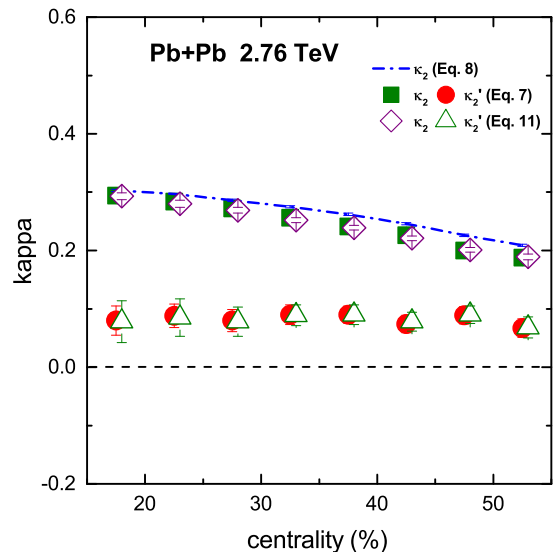


FIG. 6. (Color online) Linear and cubic order response coefficients κ_2 and κ_2' as a function of centrality percentile, from AMPT simulations of Pb-Pb collisions at $\sqrt{s_{NN}} = 2.76$ TeV. The results of κ_2 and κ_2' are calculated according to Eq. (7) and Eq. (11) corresponding to non-flow effects subtraction, respectively. For comparison, the linear response coefficient κ calculated with respect to Eq. (8) is shown as dashed line.

dynamic modelings is understandable. However, AMPT simulations contain extra event-by-event fluctuations due to non-flow effects. Even though these fluctuations are non-hydrodynamic, as they are not sensitive to dissipative effect of the medium system, they do not affect the response relations.

ACKNOWLEDGEMENTS

We thank Jean-Yves Ollitrault and Zi-Wei Lin for very helpful discussions. DXW and XGH are supported by the Young 1000 Talents Program of China, NSFC with Grant No. 11535012 and No. 11675041. LY is supported in part by the Natural Sciences and Engineering Research Council of Canada.

Appendix A: AMPT results of Pb-Pb collisions at $\sqrt{s_{NN}} = 5.02$ TeV

Recent experiments at the LHC has reached $\sqrt{s_{NN}} = 5.02$ TeV for the Pb-Pb collisions, where the fluctuations of v_2 have been measured. In this appendix, we present our results of v_2 fluctuations in terms of cumulant ratios in Fig. 7 and the standardized skewness in Fig. 8, from AMPT simulations. In the AMPT simulations for $\sqrt{s_{NN}} = 5.02$ TeV, we found that the parameter set D (see Table I) can be used to well describe the observed flow signature. Again, the observed fluctuations of v_2 are

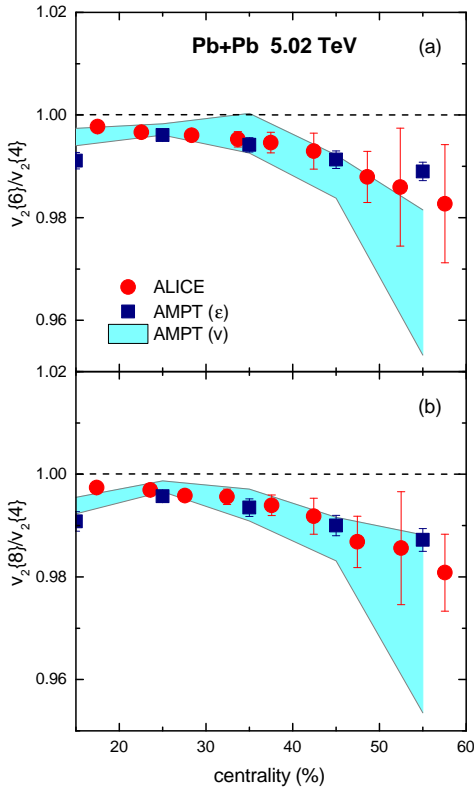


FIG. 7. (Color online) Ratios of cumulants (a) $v_2\{6\}/v_2\{4\}$ and (b) $v_2\{8\}/v_2\{4\}$ for Pb-Pb collisions at $\sqrt{s_{NN}} = 5.02$ TeV. Red points are from ALICE collaboration [24], colored bands are results of AMPT calculations. The corresponding cumulant ratios of initial ellipticity ε_2 are shown as blue squares.

found compatible with those from initial state ε_2 , implying the dominance of linear response relation between v_2 and ε_2 .

-
- [1] S. Jeon and U. Heinz, *Int. J. Mod. Phys. E* **24**, 1530010 (2015), arXiv:1503.03931 [hep-ph].
- [2] C. Gale, S. Jeon, B. Schenke, P. Tribedy, and R. Venugopalan, *Phys. Rev. Lett.* **110**, 012302 (2013), arXiv:1209.6330 [nucl-th].
- [3] C. Chattopadhyay, R. S. Bhalerao, J.-Y. Ollitrault, and S. Pal, *Phys. Rev. C* **97**, 034915 (2018), arXiv:1710.03050 [nucl-th].
- [4] S. McDonald, C. Shen, F. Fillion-Gourdeau, S. Jeon, and C. Gale, *Phys. Rev. C* **95**, 064913 (2017), arXiv:1609.02958 [hep-ph].
- [5] H. Niemi, K. J. Eskola, R. Paatelainen, and K. Tuominen, *Phys. Rev. C* **93**, 014912 (2016), arXiv:1511.04296 [hep-ph].
- [6] P. Kovtun, D. T. Son, and A. O. Starinets, *Phys. Rev. Lett.* **94**, 111601 (2005), arXiv:hep-th/0405231 [hep-th].
- [7] J.-Y. Ollitrault, *Phys. Rev. D* **46**, 229 (1992).
- [8] B. Alver and G. Roland, *Phys. Rev. C* **81**, 054905 (2010), [Erratum: *Phys. Rev. C* **82**, 039903 (2010)], arXiv:1003.0194 [nucl-th].
- [9] G. Aad *et al.* (ATLAS), *Phys. Rev. C* **90**, 024905 (2014), arXiv:1403.0489 [hep-ex].
- [10] D. Teaney and L. Yan, *Phys. Rev. C* **83**, 064904 (2011), arXiv:1010.1876 [nucl-th].
- [11] L. Yan, *Chin. Phys. C* **42**, 042001 (2018), arXiv:1712.04580 [nucl-th].
- [12] S. Acharya *et al.* (ALICE), *Phys. Lett. B* **773**, 68 (2017), arXiv:1705.04377 [nucl-ex].
- [13] L. Yan and J.-Y. Ollitrault, *Phys. Lett. B* **744**, 82 (2015), arXiv:1502.02502 [nucl-th].
- [14] G. Giacalone, L. Yan, J. Noronha-Hostler, and J.-Y. Ollitrault, *Phys. Rev. C* **95**, 014913 (2017), arXiv:1608.01823 [nucl-th].
- [15] G. Giacalone, L. Yan, J. Noronha-Hostler, and J.-Y. Ollitrault, *Phys. Rev. C* **94**, 014906 (2016), arXiv:1605.08303 [nucl-th].
- [16] Z.-W. Lin, C. M. Ko, B.-A. Li, B. Zhang, and S. Pal, *Phys. Rev. C* **72**, 064901 (2005), arXiv:nucl-th/0411110 [nucl-th].
- [17] X.-N. Wang and M. Gyulassy, *Phys. Rev. D* **44**, 3501 (1991).
- [18] B. Zhang, *Computer Physics Communications* **109**, 193 (1998).
- [19] J. Xu and C. M. Ko, *Phys. Rev. C* **83**, 034904 (2011), arXiv:1101.2231 [nucl-th].

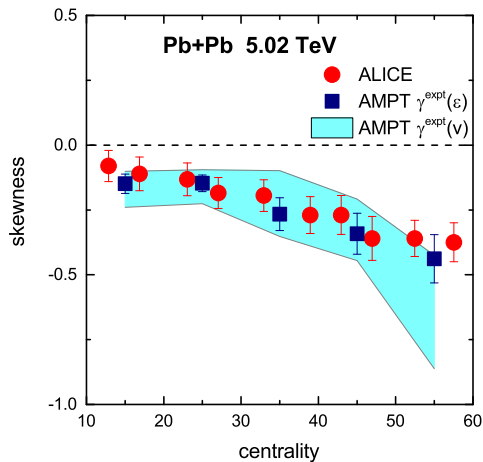


FIG. 8. (Color online) Standardized skewness of v_2 fluctuations in Pb-Pb collisions at $\sqrt{s_{NN}} = 5.02$ TeV as a function of centrality from AMPT simulations (colored band), and ALICE [24] data (red points). The corresponding results of standardized skewness of initial state ε_2 is shown as blue squares.

[20] Y. Zhang, J. Zhang, J. Liu, and L. Huo, *Phys. Rev. C* **92**, 014909 (2015).

- [21] S. Chatrchyan *et al.* (CMS), *Phys. Rev.* **C87**, 014902 (2013), [arXiv:1204.1409 \[nucl-ex\]](#).
- [22] J. Adam *et al.* (ALICE), *Phys. Rev. Lett.* **116**, 132302 (2016), [arXiv:1602.01119 \[nucl-ex\]](#).
- [23] A. M. Sirunyan *et al.* (CMS), (2017), [arXiv:1711.05594 \[nucl-ex\]](#).
- [24] S. Acharya *et al.* (ALICE), (2018), [arXiv:1804.02944 \[nucl-ex\]](#).
- [25] J. Noronha-Hostler, L. Yan, F. G. Gardim, and J.-Y. Ollitrault, *Phys. Rev.* **C93**, 014909 (2016), [arXiv:1511.03896 \[nucl-th\]](#).
- [26] F. G. Gardim, F. Grassi, M. Luzum, and J.-Y. Ollitrault, *Phys. Rev.* **C85**, 024908 (2012), [arXiv:1111.6538 \[nucl-th\]](#).
- [27] D. Solanki, P. Sorensen, S. Basu, R. Raniwala, and T. K. Nayak, *Phys. Lett.* **B720**, 352 (2013), [arXiv:1210.0512 \[nucl-ex\]](#).
- [28] J. Xu and C. M. Ko, *Phys. Rev.* **C84**, 014903 (2011), [arXiv:1103.5187 \[nucl-th\]](#).
- [29] S. Chatrchyan *et al.* (CMS), *Phys. Rev.* **C89**, 044906 (2014), [arXiv:1310.8651 \[nucl-ex\]](#).
- [30] S. Acharya *et al.* (ALICE), (2018), [arXiv:1805.04390 \[nucl-ex\]](#).
- [31] G. Aad *et al.* (ATLAS), *Eur. Phys. J.* **C74**, 3157 (2014), [arXiv:1408.4342 \[hep-ex\]](#).